

Heterodinuclear Iridium Cyclooctadiene Complexes with the [(η^5 -C₅H₅)Fe(η^6 -(1,1-di(2-propenyl)-3-butenyl)benzene)]⁺ Ligand

Silvia Marcén, M. Victoria Jiménez, Isabel T. Dobrinovich,
Fernando J. Lahoz, and Luis A. Oro*

Departamento de Química Inorgánica, Instituto de Ciencia de Materiales de Aragón,
Universidad de Zaragoza-CSIC, E-50009 Zaragoza, Spain

Jaime Ruiz and Didier Astruc*

Laboratoire de Chimie Organique et Organométallique, UMR CNRS NE 5802,
Université Bordeaux I, 351 Cours de la Libération, 33405 Talence Cedex, France

Received July 31, 2001

The X-ray crystal structure of the potentially tridentate triallyl ligand [Fe(η^5 -C₅H₅){ η^6 -(1,1-di(2-propenyl)-3-butenyl)benzene}][PF₆] ([L_{Fe}][PF₆]) (**1**) is reported. The reaction of **1** with [{Ir(μ -Cl)(cod)}₂] yields the unusual five-coordinate cationic complex [(L_{Fe})IrCl(cod)][PF₆] (**2**), for which the ¹H NMR COSY experiment and the X-ray crystal structure show the existence of two different types of allyl groups: one free noncoordinated allyl and two bonded to Ir. The reaction of **2** with silver salts gives the square-planar complex [(L_{Fe})Ir(cod)][PF₆]₂ (**3**) with the same trend of allyl coordination and displaying an NMR static behavior even at room temperature. Cyclic voltammetry of **1**, **2**, and **3** in DMF or MeCN on Pt at -40 °C shows a fully reversible Fe^{III}/Fe^{I/0} reduction wave, chemically fully irreversible Fe^{I/0} reduction wave, and Ir oxidation wave, the latter being observed only for **2**.

Introduction

The ready accessibility of the dinuclear iridium complexes [{Ir(μ -Cl)(cod)}₂]¹ and [{Ir(μ -OMe)(cod)}₂]² has promoted the development of an extensive chemistry³ of neutral and cationic square-planar complexes containing the iridium-1,5-cyclooctadiene “Ir(cod)” moiety, but only a few five-coordinate complexes containing this diolefin have been reported. This is in clear contrast with the coordination chemistry of the fluorinated diolefin tetrafluorobenzobarrelene (5,6,7,8-tetrafluoro-1,4-dihydro-1,4-ethenonaphthalene), which, due to the influence of the electron-withdrawing tetrafluorobarrelene group and, particularly, to its smaller bite angle, favors the isolation of five-coordinate complexes.⁴ Thus, although the complex [IrCl(tfb)₂] is stable,⁵ the related complex IrCl(cod)₂ dissociates in solution and dimerizes to form [{Ir(μ -Cl)(cod)}₂].⁶ These facts suggest that the tridentate olefinic complex [Fe(η^5 -C₅H₅){ η^6 -(1,1-di(2-propenyl)-3-butenyl)benzene}]⁺ ([L_{Fe}]⁺) could give dif-

ferent coordination possibilities with the “Ir(cod)” moiety, although fluxional processes might occur.

The three allyl groups were introduced in this iron-sandwich complex by CpFe⁺-induced perallylation of toluene under ambient conditions,⁷ a key reaction for the construction of dendritic cores and dendrimers in the related mesitylene case.^{7,8} In this context, complex [L_{Fe}]⁺ can be considered as a simple model to explore the transition-metal coordination at the periphery of these dendrimers containing multiple terminal triallylmethyl groups. The binding of metal cations inside or on the surface of the dendrimer structure has applications in homogeneous catalysis. In addition, the presence of reversible redox processes involving the Ir–Fe metals is relevant to the promising use of these systems as electronic switches, which adds a peculiar dimension to its organometallic chemistry.

Results and Discussion

Synthesis and Spectroscopic and Structural Characterization of the Heterodinuclear Ir–Fe Complexes. We report here on the coordination capability toward iridium of the unusual triolefin-arene iron cationic ligand, [(η^5 -C₅H₅)Fe(η^6 -(1,1-di(2-propenyl)-3-butenyl)benzene)]⁺ ([L_{Fe}]⁺). While the reaction of the [L_{Fe}][PF₆] (**1**) compound with the iridium cyclooctadiene

(1) Herde, J. L.; Lambert, J. C.; Senoff, C. V. *Inorg. Synth.* **1974**, *15*, 18.

(2) Usón, R.; Oro, L. A.; Cabeza, J. A. *Inorg. Synth.* **1985**, *23*, 126.

(3) (a) Atwood, J. D. In *Comprehensive Organometallic Chemistry*; Abel, E. W., Stone, F. G. A., Wilkinson, G., Eds.; Pergamon Press: Oxford, 1995; Vol. 8, Chapter 5.3. (b) Leigh, G. J.; Richards, R. L. In *Comprehensive Organometallic Chemistry*; Wilkinson, G., Stone, F. G. A., Abel, E. W., Eds.; Pergamon Press: Oxford, 1982; Vol. 5, Chapter 36.

(4) Esteruelas, M. A.; Oro, L. A. *Coord. Chem. Rev.* **1999**, *193*, 557.

(5) Usón, R.; Oro, L. A.; Carmona, D.; Esteruelas, M. A.; Foces-Foces, C.; Cano, F. H.; García-Blanco, S. *J. Organomet. Chem.* **1983**, *254*, 249.

(6) Onderdelinden, A. L.; Van der Ent, A. *Inorg. Chim. Acta* **1972**, *6*, 420.

(7) Moulines, F.; Djakovitch, L.; Boese, R.; Gloaguen, B.; Thiel, W.; Fillaut, J.-L.; Delville, M. H.; Astruc, D. *Angew. Chem., Int. Ed. Engl.* **1993**, *32*, 1075.

(8) Astruc, D. *Acc. Chem. Res.* **2000**, *33*, 287.

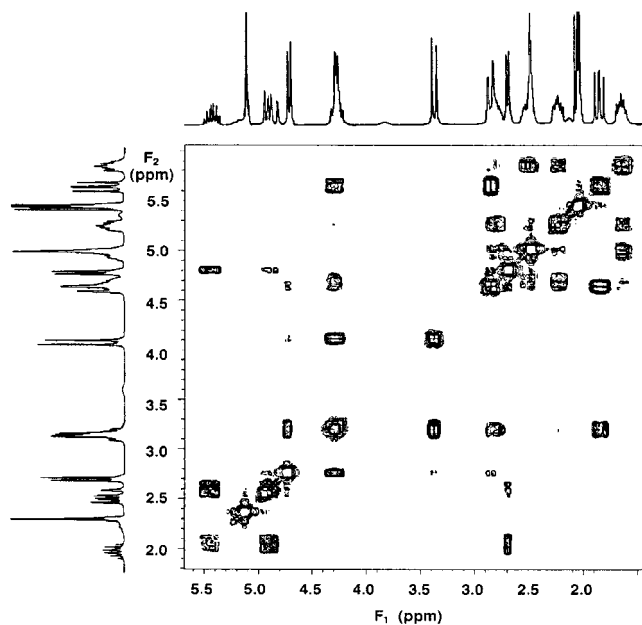
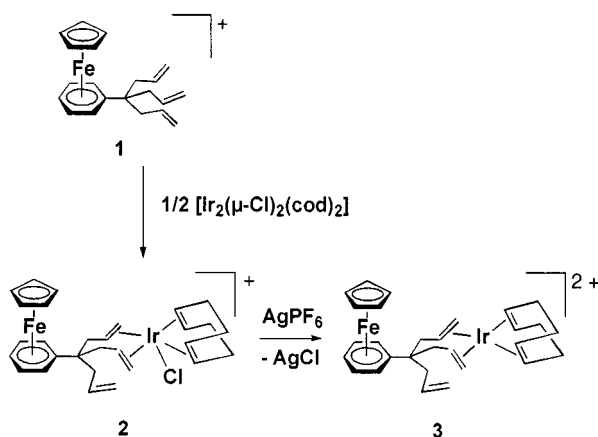


Figure 1. ^1H COSY NMR spectrum of a deuterioacetone solution of compound **2** at 293 K.

Scheme 1



dimer $[\{\text{Ir}(\mu\text{-Cl})(\text{cyclooctene})_2\}_2]$ yields an uncharacterized brown insoluble solid, the analogous reaction with $[\{\text{Ir}(\mu\text{-Cl})(\text{cod})\}_2]$ renders a yellow solid of formula $[(\text{L}_{\text{Fe}})\text{IrCl}(\text{cod})][\text{PF}_6]$ (**2**) (Scheme 1). Its formulation was assumed by the observation of the molecular ion in the FAB^+ mass spectrum.

The ^1H NMR COSY experiment (Figure 1) of a deuterioacetone solution of **2** clearly shows the existence of two different allyl groups. On one hand, a multiplet signal at δ 5.45 ppm, assigned to one vinyl proton, is observed coupled to two other vinyl protons, which are two doublet of doublets signals at δ 4.87 and 4.96 ppm, with 16.8 and 10.2 Hz coupling constants, respectively. Additionally, this multiplet is also coupled to a doublet resonance at δ 2.70 ppm belonging to the methylene protons. On the other hand, the remaining two allyl groups are related by a symmetry plane, as it is shown by integration. These two symmetry-related groups give rise to a multiplet at δ 4.30 ppm, which corresponds to two vinyl protons, coupled to the doublet signals at δ 3.38 ppm ($J_{\text{HH}} = 12.6$ Hz) and δ 4.74 ppm ($J_{\text{HH}} = 8.1$ Hz). These vinyl protons are additionally coupled to only one of the methylenic allyl protons which appears at δ 1.85 ppm ($J_{\text{HH}} = 11.1$ Hz). The latter methylenic protons

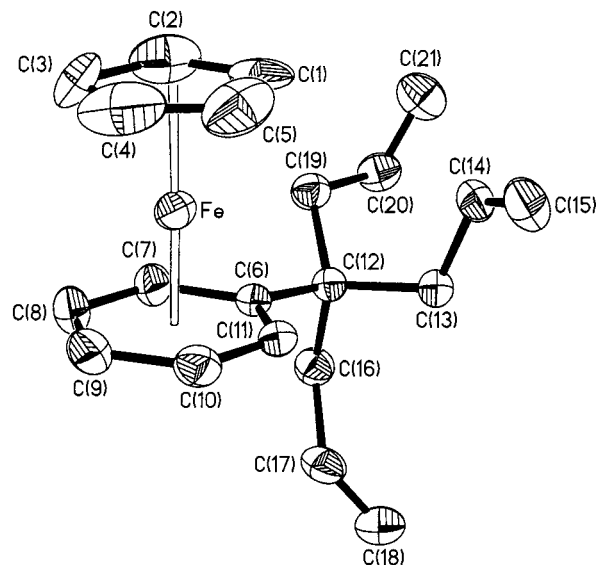


Figure 2. Molecular structure of the iron complex $[(\text{L}_{\text{Fe}})\text{PF}_6]$ (**1**).

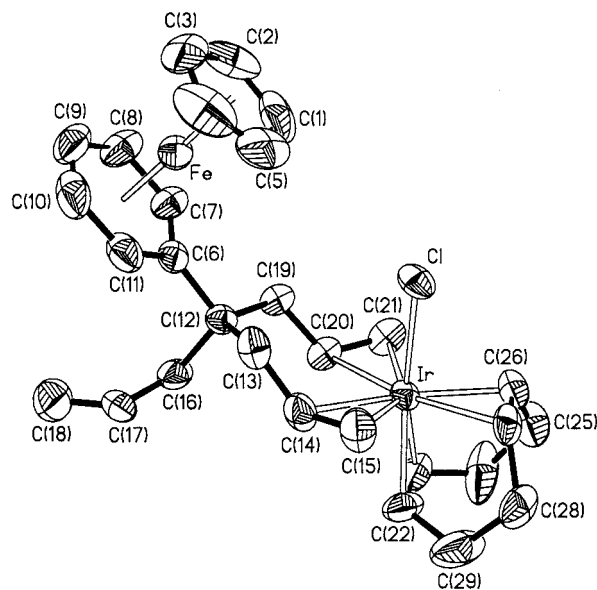


Figure 3. Molecular structure of the heterodinuclear Fe-Ir complex $[(\text{L}_{\text{Fe}})\text{IrCl}(\text{cod})][\text{PF}_6]$ (**2**).

exhibit a diastereotopic behavior and are coupled each other with a 14.4 Hz coupling constant. In conclusion, these spectroscopic data strongly support that, in a nonfluxional fashion, only two of the three terminal olefins are bonded to the iridium center, and the third one remains as a free terminal allyl group.

To obtain a better insight into the structural parameters of the new complexes, the molecular structure of the Fe-Ir heterodinuclear cation **2**, together with that of the starting triolefin-arene iron compound, $[(\text{L}_{\text{Fe}})][\text{PF}_6]$ (**1**), have been determined by X-ray diffraction (Figures 2 and 3); selected bond distances and angles for both metal complexes are collected in Table 1.

Both molecular structures show a sandwich disposition of the iron metal center between the two almost parallel planar organic rings (Cp/arene dihedral angles of $3.0(4)^\circ$ in **1** and $3.9(3)^\circ$ in **2**). The Fe-C(Cp) bond distances in complex **1** are in the range 2.038(12)–2.053(10) Å, and those to the arene ligand are between 2.089 and 2.155(2) Å. These distances are similar to

Table 1. Selected Bond Distances (Å) and Angles (deg) for the Complexes 1 and 2^a

	1	2		1	2
Fe–C(1)	2.038(12)	2.017(7)	Fe–C(6)	2.1547(17)	2.136(5)
Fe–C(2)	2.053(10)	2.012(7)	Fe–C(7)	2.0978(19)	2.077(6)
Fe–C(3)	2.050(10)	2.019(6)	Fe–C(8)	2.089(2)	2.067(7)
Fe–C(4)	2.048(12)	2.029(7)	Fe–C(9)	2.093(2)	2.072(8)
Fe–C(5)	2.044(12)	2.040(8)	Fe–C(10)	2.0873(19)	2.051(7)
Fe–G(1) ^b	1.700(6)	1.658(4)	Fe–C(11)	2.1016(17)	2.078(7)
Ir–Cl		2.3883(15)	Fe–G(2) ^b	1.5579(8)	1.535(3)
Ir–C(14)		2.319(6)	Ir–C(22)		2.168(6)
Ir–C(15)		2.236(6)	Ir–C(23)		2.169(6)
Ir–C(20)		2.268(5)	Ir–C(26)		2.162(6)
Ir–C(21)		2.191(6)	Ir–C(27)		2.167(6)
C(13)–C(14)	1.504(3)	1.481(9)	C(19)–C(20)	1.506(3)	1.502(8)
C(14)–C(15)	1.322(3)	1.386(9)	C(20)–C(21)	1.305(3)	1.393(8)
C(16)–C(17)	1.507(3)	1.492(11)	C(22)–C(23)		1.372(12)
C(17)–C(18)	1.307(3)	1.281(10)	C(26)–C(27)		1.395(9)
G(1)–Fe–G(2)	178.2(2)	178.28(19)	M(1)–Ir–M(3) ^c		99.1(2)
Cl–Ir–M(1) ^c		85.52(15)	M(1)–Ir–M(4) ^c		122.73(17)
Cl–Ir–M(2) ^c		87.77(13)	M(2)–Ir–M(3) ^c		96.77(19)
Cl–Ir–M(3) ^c		171.93(13)	M(2)–Ir–M(4) ^c		126.61(16)
Cl–Ir–M(4) ^c		87.08(14)	M(3)–Ir–M(4) ^c		84.9(2)
M(1)–Ir–M(2) ^c		109.73(17)			
C(12)–C(13)–C(14)	116.82(14)	116.5(5)	C(16)–C(17)–C(18)	125.3(2)	127.1(9)
C(13)–C(14)–C(15)	124.89(19)	122.6(7)	C(12)–C(19)–C(20)	114.60(15)	117.2(5)
C(12)–C(16)–C(17)	115.67(16)	114.7(6)	C(19)–C(20)–C(21)	124.7(2)	120.3(6)

^a For complex **1** mean values of the Fe–C distances for the disordered Cp ligand are stated. ^b G(1) and G(2) represent the centroids of the cyclopentadienyl and arene ligands, respectively. ^c M(1), M(2), M(3), and M(4) represent the midpoints of the olefinic bonds C(14)–C(15), C(20)–C(21), C(22)–C(23), and C(26)–C(27).

those already known from X-ray crystal structures of related [FeCp(arene)]⁺ complexes,^{9,10} even to those of hexaalkylbenzene complexes.^{9a,b}

The molecular structure of the Fe–Ir complex **2** is the result of the coordination of two terminal olefins of **1** to the “IrCl(cod)” moiety. The pentacoordinated saturated (18e[−]) iridium center exhibits a trigonal bipyramidal geometry, with the two apical positions being occupied by a double bond of the cyclooctadiene group (C(22) and C(23)) and the chloride ligand (Cl–Ir–M(3) 171.93(13)°); bond angles in the equatorial plane range between 109.73(17) and 126.61(16)°. If compared with **1**, complex **2** displays a significant elongation of the two coordinated C–C double bonds from a mean value of 1.311(2) Å in **1** to 1.391(7) Å; the remaining noncoordinated olefinic bond (C(17)–C(18)) presents an identical bond length in both structures **1** and **2**, 1.281(10) Å, also similar to that reported in the free nonaallyl arene derivative 1,3,5-{C(CH₂CHCH₂)₃}C₆H₃ obtained by nonaallylation of mesitylene.⁷ Another striking structural parameter in **2** is the long Ir–C distances observed for the two coordinated olefins of the L_{Fe} ligand. Although the C=C bond lengths of the four coordinated olefins in **2** exhibit identical values, the Ir–C bond separations clearly differ, showing significantly longer bond distances for the allylic carbons (mean 2.254(3) Å) than for the cyclic diolefin (2.167(3) Å).

(9) For a few examples of X-ray crystal structures of [Fe(η⁵-C₅H₅)-(η⁶-arene)]⁺ derivatives, see: (a) Hamon, J.-R.; Saillard, J.-Y.; Le Beuze, A.; McGlinchey, M.; Astruc, D. *J. Am. Chem. Soc.* **1982**, *104*, 7549. (b) Fillaut, J.-L.; Boese, R.; Astruc, D. *Synlett* **1992**, 55. (c) Subramanian, S.; Wang, L.; Zaworotko, M. *Organometallics* **1993**, *12*, 310. (d) Ishii, Y.; Kawaguchi, M.; Ishino, Y.; Aoki, T.; Hidai, M. *Organometallics* **1994**, *13*, 5062. (e) Manzur, C.; Baeza, E.; Millan, L.; Fuentealba, M.; Hamon, P.; Hamon, J.-R.; Boys, D.; Carrillo, D. *J. Organomet. Chem.* **2000**, *608*, 126.

(10) For a reference gathering a large number of interatomic and metal–ligand distances obtained from the Cambridge Crystallographic Data Base Center, see: Orpen, A. G.; Brammer, L.; Allen, F. H.; Kennard, O.; Watson, D. G.; Taylor, R. *J. Chem. Soc., Dalton Trans.* **1989**, S1.

Although nonstatistically significant, most of the Fe–C(Cp) and Fe–C(arene) bond distances in **2** seem to show a tendency toward shorter lengths if compared with **1**, probably reflecting the electron density release from the terminal olefins of the iron metalloligand after coordination to the Ir center. This electron density release would be consequently compensated with a stronger interaction between the donor aromatic rings (Cp and arene) and the iron metal.

It seems interesting to stress that the trioлеfin-arene iron cationic ligand, [L_{Fe}]⁺ favors the formation of the unusual five-coordinate cationic complex [(L_{Fe})IrCl(cod)]-[PF₆][−] (**2**), most probably due to its peculiar weak donor capacities as visualized from the structural parameters (Ir–C bond distances).

Complex **2** reacts with silver salts to yield complex [(L_{Fe})Ir(cod)][PF₆]₂ (**3**). Elemental analysis and mass spectrum show the loss of the chloride ligand from the precursor complex **2**, and in agreement with this, acetone solutions of compound **3** behave as 1:2 electrolytes. The ¹H NMR spectrum is analogous to that of **2** showing only two of the three olefins of the [L_{Fe}]⁺ cationic ligand coordinated. All these data are in accordance with a square-planar coordination for the iridium center in **3** (Scheme 1). Although this complex is a potential candidate to display a fluxional behavior involving the three olefins of the cation, the heterodinuclear complex shows a static behavior even at room temperature. Further work on the coordination capability of the metalloligand [(η⁵-C₅H₅)Fe(η⁶-(1,1-di(2-propenyl)-3-butenyl)benzene)]⁺ is in progress.

Electrochemistry. The [FeCp(arene)]⁺ complexes are known for their interesting redox behavior.^{11,12} It is of interest to examine now the mutual influence of

(11) Astruc, D. *Electron Transfer and Radical Reactions in Transition-Metal Chemistry*, VCH: New York, 1995; Chapter 2, pp 147–149.

(12) Hamon, J.-R.; Astruc, D.; Michaud, P. *J. Am. Chem. Soc.* **1981**, *103*, 758.

Table 2. Crystal Data and Data Collection and Refinement for Complexes 1 and 2

	1	2
chem formula	C ₂₁ H ₂₅ F ₆ FeP	C ₂₉ H ₃₇ ClF ₆ FeIrP
fw	478.23	814.06
cryst size, mm	0.62 × 0.48 × 0.43	0.49 × 0.23 × 0.21
cryst syst	monoclinic	monoclinic
space group	<i>P</i> 2 ₁ / <i>n</i>	<i>P</i> 2 ₁ / <i>n</i>
<i>a</i> , Å	9.377(2)	13.1952(19)
<i>b</i> , Å	17.632(4)	15.322(3)
<i>c</i> , Å	13.063(3)	13.999(2)
α, deg	106.823(17)	92.598(12)
<i>V</i> , Å ³	2067.3(8)	2827.3(7)
<i>Z</i>	4	4
<i>D</i> _{calcd} , g cm ⁻³	1.537	1.912
μ, mm ⁻¹	0.864	5.425
no. of measd reflns	9390	7352
no. of unique reflns	5957 (<i>R</i> _{int} = 0.0469)	5564 (<i>R</i> _{int} = 0.0138)
min., max. transm factor	0.544, 0.614	0.318, 0.394
no. of data/restraints/params	5957/10/309	5564/1/389
<i>R</i> (<i>F</i>) (<i>F</i> ² ≥ 2σ(<i>F</i> ²))	0.0393	0.0341
<i>wR</i> (<i>F</i> ²) (all data)	0.0937	0.0850

^a *R*(*F*) = Σ|*F*_o − |*F*_c||Σ|*F*_o| for 4541 (**1**) and 4413 (**2**) observed reflections. ^b *wR*(*F*²) = (Σ[*w*(*F*_o² − *F*_c²)²]/Σ[*w*(*F*_o²)²])^{1/2}.

Table 3. Cyclic Voltammetry Data for the Complexes 1–3^a

	solvent	1st reduction (V)	2nd reduction (V)	oxidation (V)
1	DMF	−1.81	−2.75	>1
	MeCN	−1.79		>1.3
2	DMF	−1.82	−2.75	>1
	MeCN	−1.81		1.00
3	DMF	−1.86		>1
	MeCN	−1.84		>1.3

^a Redox potentials vs [FeCp₂]^{0/+} (internal reference) recorded for the complexes **1**, **2**, and **3** determined by cyclic voltammetry (see the Experimental Section) in DMF or MeCN on Pt at −40 °C. The average between the reduction and oxidation peaks (*i*_a/*i*_c = 1 for **1–3**) is reported in this table for the first reduction (ΔE was 50 mV for **1–3**, consistent with a fast single-electron transfer), whereas the potential peak values of the irreversible processes at a scan rate of 200 mV s⁻¹ are given for the 2nd reduction wave (*i*_a/*i*_c = 0 for **1–3**) and for the oxidation wave (*i*_c/*i*_a = 0 for **1–3**).

the two metal centers using electrochemistry. In particular, one can scrutinize this mutual influence in terms of thermodynamics via the redox potentials and the stability of the odd redox states via the shapes of the cyclovoltammetry waves. The difference of charge between the two heterodinuclear compounds, due to the formally neutral (**2**) or cationic (**3**) iridium moieties, is also of interest from the electrochemical point of view. Indeed, the doubly positively charged complex **3** should be more difficult to oxidize and easier to reduce than the monopositively charged complex **2**.

Cyclovoltammograms were recorded for the three complexes **1**, **2**, and **3** at −40 °C in both DMF and MeCN using Pt as working and counter-electrode, and one of silver as reference electrode. Values of the reduction and oxidation potentials and information concerning the reversibilities are gathered in Table 3.

The first reduction wave of **1**, **2**, and **3** corresponds to the single-electron reduction of the d⁶, Fe^{II}, 18-electron complexes to the d⁷, Fe^I, 19-electron species.^{11,12} Their redox potentials are in the expected range and show almost the same value for the three compounds, which indicates that the electronic influence of the added iridium moiety on the iron center is negligible. This

feature is not surprising because no conjugation is involved between the two metal centers. The cyclovoltammograms recorded at room temperature show a reduced chemical reversibility, which indicates that the 19-electron species is not stable for **1–3**, whereas the parent 19-electron compound [FeCp(C₆H₆)] can be isolated as a forest-green powder.^{12,13} Such a situation is encountered when the arene ring bears bulky substituents because the weakening of the metal–ligand bond by addition of an electron in an antibonding orbital (*e*₁^{*}) is responsible for the fragilization when the steric factor comes in synergy.¹⁴ The problem is much more dramatic and is fully apparent at −40 °C for the second single-electron-transfer reduction which is reversible with the parent compound [FeCp(C₆H₆)] at −40 °C and completely irreversible here for the three compounds **1**, **2**, and **3**. There are now two electrons in the antibonding orbitals *e*₁^{*} in the 20-electron species, which explains the enhanced instability when bulk is present nearby. As indicated by the 50 mV value at −40 °C for the difference in potentials between the cathodic and anodic peak (ΔE_p), the heterogeneous electron transfer is fast between the Pt electrode and the organoiron group, whose sandwich structure does not change much in the course of electron transfer. Although this is also usually the case for the second reduction wave of this family of compounds, it is not apparent here because of the complete chemical irreversibility of this second wave. No reduction wave was observed for the iridium groups up to −3 V vs FeCp₂^{0/+}, even in the case of **3**, which bears a cationic charge on the iridium center and should therefore be easier to reduce than the neutral iridium group of **2**. On the oxidation side, the iridium systems are also usually rather poor. Likewise, the oxidation of Fe^{II} to Fe^{III} is usually not observed in such complexes, because the positive charge on the iron center displaces this oxidation to much higher potentials, beyond 2 V. The compound **3** could indeed not be oxidized up to 1.3 V vs FeCp₂^{0/+} (e.g., 1.7 V vs SCE). A chemically irreversible oxidation wave was found for **2**, however, at +1 V vs in MeCN. The irreversible character of this wave at such a low temperature precludes further analysis of the redox system at this stage.

Experimental Section

Physical Measurements. Infrared spectra were recorded as Nujol mulls on polyethylene sheets using a Nicolet 550 spectrometer. C, H, and N analyses were carried out in a Perkin-Elmer 2400 CHNS/O analyzer. NMR spectra were recorded on a Varian Gemini 2000, 300 MHz spectrometer. ¹H and ¹³C NMR chemical shifts were measured relative to partially deuterated solvent peaks but are reported in ppm relative to tetramethylsilane. ³¹P and ¹⁹F NMR chemical shifts were measured relative to H₃PO₄ (85%) and CFCl₃, respectively. Coupling constants, *J*, are given in hertz. Generally, spectral assignments were achieved by ¹H COSY and ¹³C DEPT experiments. MS data were recorded on a VG Autospec double-focusing mass spectrometer operating in the positive mode. Ions were produced with a Cs⁺ gun at ca. 30 kV, and 3-nitrobenzyl alcohol (NBA) was used as the matrix. Conductivities were measured in ca. 3 × 10⁻⁴ M solutions using a

(13) Nesmeyanov, A. N.; Vol'kenau, N. A.; Shilovstseva, L. S. *J. Organomet. Chem.* **1973**, *61*, 329.

(14) Hamon, J.-R.; Hamon, P.; Boukheddaden, K.; Linares, J.; Varet, F.; Astruc, D. *Inorg. Chem. Acta* **1995**, *240*, 105.

Philips PW 9501/01 conductimeter. The cyclic voltammograms were recorded on a PAR 273 potentiostat galvanostat. Care was taken in the CV experiments to minimize the effects of solution resistance on the measurements of peak potentials. Therefore, the use of positive feedback *iR* compensation and dilute solution (10^{-3} M) maintained currents between 1 and 10 μ A. The additional redox couple $[\text{FeCp}_2]^{0/+}$ was used as a control of *iR* compensation. The reference electrode was an Ag quasi-reference electrode (QRE). The silver wire was pretreated in 10 M HNO_3 for 5 min before use. The value of the $[\text{FeCp}_2]^{0/+}$ redox couple was 0.382 V vs SCE on Pt in MeCN and 0.475 V vs SCE on Pt in DMF. The QRE was calibrated by adding the $[\text{FeCp}_2]^{0/+}$ reference couple. The counter-electrode was platinum. The scan rate was 200 mV s^{-1} .

Synthesis. $[(\eta^5\text{-C}_5\text{H}_5)\text{Fe}(\eta^6\text{-}(1,1\text{-di}(2\text{-propenyl)}\text{-3-butenyl)-\text{benzene}))][\text{PF}_6]$ ($[\text{L}_{\text{Fe}}][\text{PF}_6]$) (**1**) was prepared following the procedure described in ref 7. All reactions were carried out with exclusion of air and light by using standard Schlenk techniques. Solvents were dried by known procedures and distilled under argon prior to use.

Preparation of $[(\text{L}_{\text{Fe}})\text{IrCl}(\text{cod})][\text{PF}_6]$ (2**).** A solution of $[(\eta^5\text{-C}_5\text{H}_5)\text{Fe}(\eta^6\text{-}(1,1\text{-di}(2\text{-propenyl)}\text{-3-butenyl)-\text{benzene}))][\text{PF}_6]$ ($[\text{L}_{\text{Fe}}][\text{PF}_6]$) (**1**) (71.2 mg, 0.149 mmol) in acetone (5 mL) was treated with $[\text{Ir}_2(\mu\text{-Cl})_2(\text{cod})_2]$ (50 mg, 0.074 mmol), and the mixture was stirred for 2 h. The resulting yellow solution was concentrated to ca. 0.5 mL, and diethyl ether was added to precipitate a yellow solid. The solution was decanted, and the solid was washed several times with diethyl ether and dried in vacuo. Crystals were obtained by slow diffusion of diethyl ether into a concentrated solution of the complex in acetone: yield 111 mg (92%); $^1\text{H NMR}$ (acetone- d_6 , 293) δ 1.65 (m, 2H, $>\text{CH}_2$, cod), 1.85 (dd, $J_{\text{HH}} = 11.1$, $J_{\text{HH}} = 14.4$, 2H, $>\text{CH}_2$, allyl), 2.24 (m, 2H, $>\text{CH}_2$, cod), 2.50 (br, 2H, =CH, cod), 2.54 (m, 2H, $>\text{CH}_2$, cod), 2.70 (d, $J_{\text{HH}} = 7.5$, 2H, $>\text{CH}_2$, allyl), 2.80 (m, 2H, $>\text{CH}_2$, cod), 2.86 (d, $J_{\text{HH}} = 14.4$, 2H, $>\text{CH}_2$, allyl), 3.38 (d, $J_{\text{HH}} = 12.6$, 2H, =CH₂, allyl), 4.30 (m, 4H: 2H =CH allyl, 2H, =CH, cod), 4.74 (d, $J_{\text{HH}} = 8.1$, 2H, =CH₂, allyl), 4.87 (dd, $J_{\text{HH}} = 16.8$, $J_{\text{HH}} = 2.1$, 1H, =CH₂, allyl), 4.96 (dd, $J_{\text{HH}} = 10.2$, $J_{\text{HH}} = 2.1$, 1H, =CH₂, allyl), 5.14 (s, 5H, Cp), 5.45 (m, 1H, =CH, allyl), 6.46 (m, 5H, C₆H₅, benzene); $^{13}\text{C}\{^1\text{H}\}$ NMR (acetone- d_6 , 293) δ 31.87, 33.55 (both s, $>\text{CH}_2$, cod), 34.26, 42.36 (both s, $>\text{CH}_2$, allyl), 47.86, 54.64 (both s, =CH₂, allyl), 66.57, 69.52 (both s, =CH, cod), 77.50 (s, Cp), 82.78 (s, =CH, allyl), 86.40, 87.79, 88.30 (all s, CH, C₆H₅), 117.39 (s, C, C₆H₅), 119.73 (s, C, allyl), 133.63 (s, =CH, allyl); Λ_{M} (5×10^{-4} M, acetone) 121 $\Omega^{-1} \text{cm}^2 \text{mol}^{-1}$ (1:1); MS(FAB+) *m/z* (%) 669 (10) [M^+], 333 (100) [L_{Fe}]. Anal. Calcd for C₂₉H₃₇FeIrClPF₆: C, 42.79; H, 4.58. Found: C, 43.14; H, 4.88.

Preparation of $[(\text{L}_{\text{Fe}})\text{Ir}(\text{cod})][\text{PF}_6]_2$ (3**).** A solution of $[(\text{L}_{\text{Fe}})\text{IrCl}(\text{cod})][\text{PF}_6]$ (**2**) (108 mg, 0.133 mmol) in acetone was treated with AgPF₆ (33.5 mg, 0.133 mmol) with exclusion of light. The suspension was stirred for 1 h, and the AgCl formed was filtered. The resulting yellow solution was concentrated to ca. 1 mL, and a yellow solid was obtained by addition of diethyl ether. The solid was washed several times with diethyl ether and vacuum-dried: yield 104 mg (85%); $^1\text{H NMR}$ (acetone- d_6 , 293) δ 1.30 (dd, $J_{\text{HH}} = 14.1$, $J_{\text{HH}} = 3.0$, 2H, $>\text{CH}_2$, allyl), 1.53 (m, 2H, $>\text{CH}_2$, cod), 2.19 (m, 2H, $>\text{CH}_2$, cod), 2.51 (m, 2H, $>\text{CH}_2$, cod), 2.61 (m, 2H, =CH, cod), 2.79 (d, $J_{\text{HH}} = 7.5$, 2H, $>\text{CH}_2$, allyl), 2.80 (d, $J_{\text{HH}} = 12.0$, 2H, =CH₂, allyl), 2.87 (m, 2H, $>\text{CH}_2$, cod), 3.38 (d, $J_{\text{HH}} = 14.1$, 2H, $>\text{CH}_2$, allyl), 4.38 (m, 2H =CH allyl), 4.72 (m, 2H, =CH, cod), 4.91 (d, J_{HH}

= 8.1, 2H, =CH₂, allyl), 4.96 (d, $J_{\text{HH}} = 11.4$, 1H, =CH₂, allyl), 5.09 (s, 5H, Cp), 5.26 (d, $J_{\text{HH}} = 15.6$, 1H, =CH₂, allyl), 5.46 (m, 1H, =CH, allyl), 6.49 (m, 5H, C₆H₅, benzene); $^{13}\text{C}\{^1\text{H}\}$ NMR (acetone- d_6 , 293) δ 30.27, 33.27 (both s, $>\text{CH}_2$, cod), 34.65, 40.82 (both s, $>\text{CH}_2$, allyl), 47.85, 56.47 (both s, $>\text{CH}_2$, allyl), 67.73, 71.26 (both s, =CH, cod), 75.10 (s, Cp), 76.81 (s, =CH, allyl), 85.69, 87.30, 87.95 (all s, CH, C₆H₅), 116.91 (s, C, C₆H₅), 119.41 (s, C, allyl), 133.15 (s, =CH, allyl); Λ_{M} (5×10^{-4} M, acetone) 168 $\Omega^{-1} \text{cm}^2 \text{mol}^{-1}$ (1:2); MS(FAB+) *m/z* (%) 634 (30) [M^+], 333 (80) [L_{Fe}]. Anal. Calcd for C₂₉H₃₇FeIrP₂F₁₂: C, 37.71; H, 4.04. Found: C, 37.35; H, 4.35.

Crystal Structure Determination of Complexes **1** and **2**

A summary of crystal data collection and refinement parameters for the two structural analyses is reported in Table 2. A yellow (**1**) and a light yellow (**2**) crystal were glued to glass fibers and mounted on Siemens P4 (**1**) and Siemens-Stoe AED-2 (**2**) diffractometers equipped with graphite-monochromated Mo K α radiation ($\lambda = 0.71073$ Å) and low-temperature equipment (150 K). Cell constants were obtained from the least-squares fit on the setting angles of 58 reflections in the range $24.8^\circ \leq 2\theta \leq 44^\circ$ for **1** and 54 reflections in the range $20^\circ \leq 2\theta \leq 35^\circ$ for **2**. Three standard reflections were monitored throughout data collection every 97 measured reflections (**1**), or every 55 min of measuring time (**2**), to check crystal and instrument stability; no significant variations of the intensities were observed. All data were corrected for Lorentz and polarization effects. A semiempirical absorption correction using a ψ -scan method¹⁵ was applied for **1** and a numerical face-based absorption correction for **2**.¹⁶

The structures were solved by direct methods and subsequent difference Fourier techniques and refined by full-matrix least-squares methods on F^2 (SHELXL-97)¹⁷ with initial isotropic thermal parameters. Anisotropic thermal parameters were used in the last cycles of refinement for all non-hydrogen atoms in both structures. In **1**, a model for the disorder of the cyclopentadienyl ligand (two moieties, 0.6 and 0.4 occupancies) had to be included. Hydrogen atoms were found from difference Fourier maps or placed in calculated positions (for the disordered cyclopentadienyl ligand) and refined riding on carbon atoms. Atomic scattering factors were used as implemented in the program.¹⁷

Acknowledgment. We thank the Ministerio de Ciencia y Tecnología (MCYT-PNI-BQU2000-1170), the Institut Universitaire de France (IUF), the CNRS, and the Université Bordeaux I for financial support. I.T.D. thanks Gobierno de Aragón for a grant.

Supporting Information Available: Listings of atomic coordinates, hydrogen positional parameters, isotropic and anisotropic displacement parameters, and complete bond distances and angles for compounds **1** and **2**. This material is available free of charge via the Internet at <http://pubs.acs.org>.

OM010684Z

(15) North, A. C. T.; Phillips, D. C.; Mathews, F. S. *Acta Crystallogr., Sect. A* **1968**, *24*, 351.

(16) *XPREP Program* (v. 5.03); Siemens Analytical X-ray Instruments, Inc.: Madison, WI, 1994. The morphology of the crystal was defined by the faces 1 1 0, $-1-1 0$ (0.21 mm); $-1 1 0$, $1-1 0$ (0.21 mm); 0 0 1, 0 0-1 (0.46 mm).

(17) Sheldrick, G. M. *SHELXL-97*, Program for Crystal Structure Refinement; University of Göttingen: Göttingen, Germany, 1997.